Tensile deformation of poly(*p*-phenylene terephthalamide) fibres, an experimental and theoretical analysis

M. G. Northolt
Akzo Research Laboratories, Corporate Research Department, 6824 BM Arnhem, the Netherlands
(Received 20 February 1980)

The tensile deformation of poly(*p*-phenylene terephthalamide) fibres has been investigated. Functional relationships observed between stress, crystallite orientation distribution, dynamic modulus and strain are derived from an analysis of the deformational behaviour of a series model consisting of a linear arrangement of crystallites. It is shown that the deformation of these fibres is largely brought about by the elastic strain and irreversible rotation of the crystallites. A formula is derived for the stress–strain relationship of a crystalline polymeric fibre with a narrow crystallite orientation distribution.

INTRODUCTION

The mechanical and structural changes during extension of wholly paracrystalline fibres have been investigated. In a previous paper[1] a single-phase paracrystalline model was proposed for poly(*p*-phenylene terephthalamide) fibres (PpPTA) which resulted in an interpretation of the linear relation observed between the dynamic extensional compliance at zero strain and the orientation distribution parameter, $\langle \sin^2 \varphi \rangle$, of the crystallite symmetry axis. In this series model the fibre is regarded as being built up of parallel aligned fibrils in which crystallites having a narrow orientation distribution relative to the fibre axis are linked end-to-end. This structural model agrees well with the results of various X-ray and electron diffraction studies[1,2]. We will show that a further development of the series model yields the functional relationships which have been observed between stress, strain and crystallite orientation distribution during extension of the fibre. Our study is limited to medium and highly oriented fibres of PpPTA.

EXPERIMENTAL

The tensile behaviour of PpPTA fibres and the accompanying structural changes have been investigated by means of measurements of the dynamic modulus and the crystallite orientation distribution during simple extension. The test samples in the various experiments consisted of non-twisted multifilament yarns of a thousand filaments, bundles of only a few filaments, as well as monofilaments of about 13 μm diameter. It was ascertained that the results obtained from the multifilaments were typical of the single filaments. *Table* 1 presents the ordinary mechanical properties and the density of the four different fibres investigated in this study. The density was measured by the submerged cantilever method[3]. The strength, elongation at break and the initial static modulus given in this Table were measured with an Instron Tensile Tester, Model 1112, on non-twisted multifilaments using a test length of 50 cm and a strain rate of 10% min^{-1}. All strain measurements on multifilament bundles were performed with a bonded strain gauge extensometer.

We will first discuss some general features of the tensile curve which is shown schematically in *Figure* 1. The numbers in this Figure indicate what is meant by the first and the second extension of the fibre. For strain rates larger than about 5% min^{-1} the shape of the curve is almost a straight line, being slightly convex at large extensions. At lower strain rates the curve adopts a sigmoid shape, particularly in the case of fibres with a relatively low initial modulus. The decrease in slope begins near 0.4% strain. Hysteresis is not clearly observed until the strain in the first extension cycle has reached about 0.4%. Typical values for the residual deformation or set range from 0.14% for a strain of 1.0% to about 0.8% for a strain of 2.7%. The residual deformation incurred in the second and higher cycles is small, being of the order of 0.02% at a strain of 2.0%. For strains exceeding the maximum strain in the first cycle, the curve will follow the original curve. The initial slope of the descending part at the point of reversal of the strain cycle has a value close to the dynamic modulus at that point. The stress relaxation is small, preliminary measurements yielded the relation

$$\sigma_t = \sigma_1 t^{-m}$$

Table 1 Densities and tensile properties of PpPTA fibres measured on non-twisted multifilaments

Fibre	Density (kg m^{-3})	Strength (GN m^{-2})	Elongation at break (%)	Static modulus (GN m^{-2})
1	1447	2.12	2.64	76
2	1458	1.96	2.83	66
3	1450	1.57	2.82	55
4	1446	2.20	2.17	105

0032-3861/80/101199-06$02.00

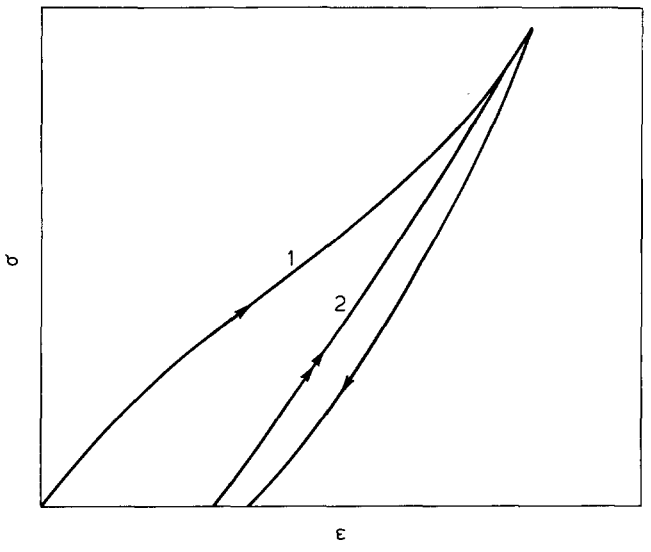

Figure 1 Schematic representation of the tensile curve measured at low strain rates

where σ_1 and σ_t are the stresses at 1 and t min relaxation time. For fibre 2 the values $m=0.0145$ was found at a strain of 2.0%.

The change of the crystallite orientation distribution in a multifilament yarn as a function of stress and strain was measured by taking an X-ray diffraction pattern after each stepwise increase in stress. The creep during the exposure of 30 min was less than 5% of the observed strain level. The orientation distribution parameter of the crystallite principal axis is defined as:

$$\langle \sin^2\varphi \rangle = \frac{\int_0^{\pi/2} \rho(\varphi)\sin^3\varphi \mathrm{d}\varphi}{\int_0^{\pi/2} \rho(\varphi)\sin\varphi \mathrm{d}\varphi}$$

where φ is the disorientation angle relative to the fibre axis. This parameter was determined from densitometer traces of the azimuthal profile of the (200) equatorial reflection. The azimuthal profile can be fitted to a Lorentz-IV distribution:

$$\rho(\varphi') = \frac{\rho(0)}{(1+p^2\sin^2\varphi')^4}$$

where

$$p^2 = \frac{0.1892}{\sin^2\varphi'_h}$$

and $2\varphi'_h$ is the width at half-height. Next it can then be derived that for the fibres concerned the value for $\langle \sin^2\varphi \rangle$ of the crystallite orientation distribution parameter with respect to the fibre axis may be approximated by:

$$\langle \sin^2\varphi \rangle = \frac{0.4}{p^2}$$

Inherent to the definition of $\langle \sin^2\varphi \rangle$ is the large weight given to the tail ends of the orientation distribution profile. This part of the profile, however, has the lowest experimental precision. Hence, the uncertainty in the level of the baseline in conjunction with the possible presence of adjacent reflections leads to an estimated error of 10% for small values to about 5% for the large values of this orientation parameter. *Figure* 2 presents the orientation parameter as a function of the applied stress during extension of the fibre, and shows an exponential relationship. *Figure* 3 displays the strain as a function of $\langle \sin^2\varphi \rangle$.

The dynamic tensile modulus, E, was measured as a function of strain and stress using the pulse propagation technique. The method is based on the propagation of longitudinal acoustic waves in the filament with a duration of 100 μs and a frequency of 100 pulses per second. The pulses are generated by a piezoelectric crystal, is in contact with the yarn. The travelling time of

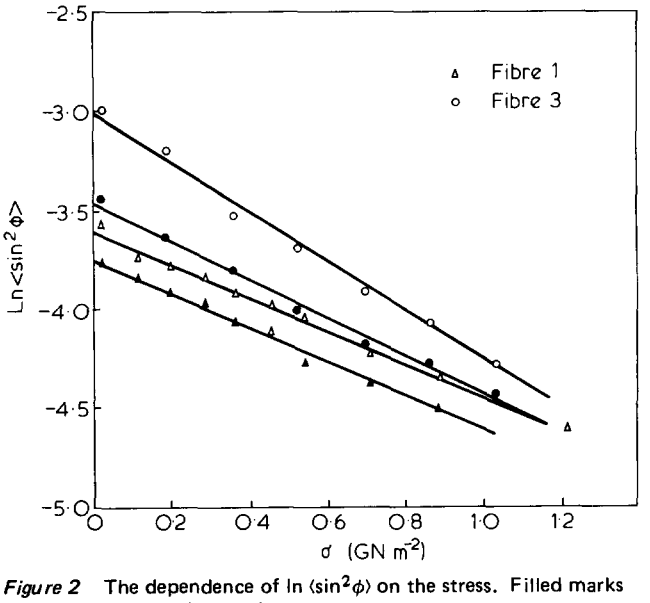

Figure 2 The dependence of ln $\langle \sin^2\phi \rangle$ on the stress. Filled marks designate the second extension

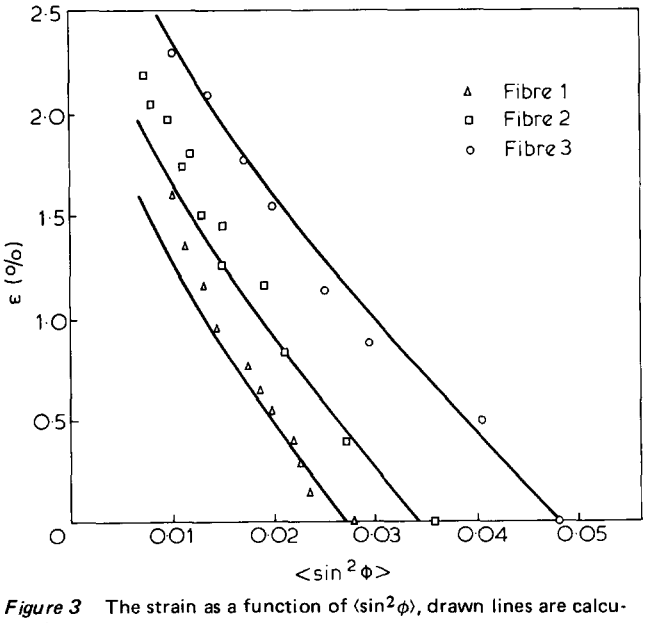

Figure 3 The strain as a function of $\langle \sin^2\phi \rangle$, drawn lines are calculated curves

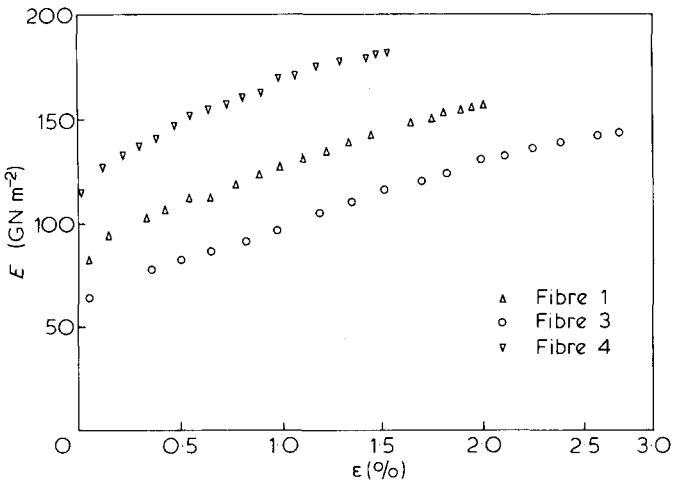

Figure 4 Dependence of the dynamic modulus on the strain

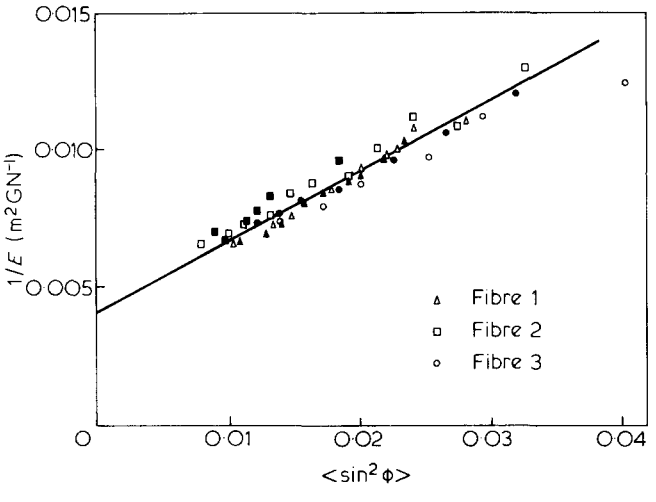

Figure 5 Dependence of the dynamic compliance on $\langle \sin^2\phi \rangle$ during extension of the fibre. Open marks for the first extension, filled marks for the second extension

the pulse over a known distance is calculated from the delay between the pulse emitted by the first crystal and the reception of this pulse by the second and similar crystal. Corrections have been made for the delay of the transmitting crystal. Since neglect of attenuation in the fibre is permitted, the dynamic modulus is given by the Laplace equation $E = \rho c^2$, where ρ is the density of the fibre and c the travelling speed. As for the orientation measurements the load was increased stepwise after a constant time interval during which E was measured. The time intervals were chosen to be equal to the X-ray exposure time, but also much shorter. Due to the waviness of the filaments the value of E at zero strain could not be properly measured, so it was derived from extrapolation between 0.2 and 0.5% strain. The dynamic or so-called sonic modulus as a function of the strain observed on multifilament yarn in the first extension is depicted in *Figure* 4. The relation between dynamic extensional compliance and $\langle \sin^2\varphi \rangle$ during extension has been derived from the measurements of the orientation distribution and the dynamic modulus as a function of the stress. The observations for the first as well as the second extension are given in *Figure* 5.

The values of E measured by the pulse propagation technique were found to be equal to those obtained by applying a small sinusoidal tensile strain. Using a Rheovibron DDV-II, these measurements at 0.01, 0.1, 1.0 and 3.5 Hz did not show any frequency dependence of the modulus at room temperature. Measurements performed at 10 kHz using the standing longitudinal wave technique likewise gave the same results.

The residual deformation (ε_p) was measured as a function of the stress for loading and relaxation times of 5 min. The data are presented in *Figure* 6.

INTERPRETATION

From wide and small-angle X-ray diffraction studies it is known that the PpPTA fibres are built up of fibrils running parallel to the fibre axis. The fibrils are considered to be chains of crystallites arranged end to end. Here the crystallites are assumed to be cylindrically symmetric bodies whose symmetry axes have an orientation distribution with the applied stress directed along the fibre axis. The dimensions of the crystallites calculated from X-ray diffraction data are about 5 nm normal to the symmetry axis and about 25 nm along this axis.

In this study we have investigated only medium and highly oriented fibres, for which the crystallite orientation distribution has a width of less than 20 degrees at half-height. For these fibres a linear relation between the initial compliance, as determined by the wave propagation method, and the orientation parameter $\langle \sin^2\varphi \rangle$ was observed and found to be in accordance with the results derived from an analysis of the series model of aggregates[1]:

$$S_{33} = \frac{1}{e_3} + A\langle \sin^2\varphi \rangle \qquad (1)$$

where A, in amended form, is given by:

$$A = \frac{1}{g} - \frac{2(1+\nu_{13})}{e_3} \qquad (2)$$

In these expressions e_3 is the elastic modulus of the crystallite parallel to its axis of symmetry, g the shear modulus in a plane containing the symmetry axis, and ν_{13} is the Poisson ratio for a stress along this axis. We note here that expression (2) presents a measure of the anisotropy of the crystallites, since for an isotropic body $g = e/2(1+\nu)$. *Figure* 5 shows the observed dynamic compliances *versus* $\langle \sin^2\varphi \rangle$ during the first and the second

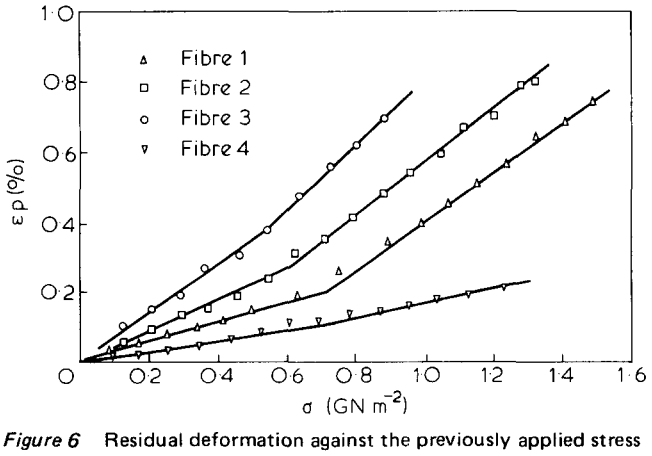

Figure 6 Residual deformation against the previously applied stress

Table 2 Values of C (m^2 GN^{-1}) from the orientation (a) and the dynamic (b) modulus measurements as a function of the stress. Subscript refers to the drawing cycle. C_1' for $\sigma > 0.8$ GN m^{-2}

		(a)		(b)		
Fibre	$\langle\sin^2\phi_0\rangle$	C_1	C_2	C_1	C_2	C_1'
1	0.027(1)	0.87(5)	0.88(5)	0.83(3)	0.76(3)	0.52(2)
2	0.033(1)	1.08(4)	0.89(5)	0.99(2)	0.90(2)	0.52(4)
3	0.048(2)	1.28(5)	0.98(5)	1.09(3)	0.99(3)	0.58(3)
4	0.016(1)	–	–	0.81(3)	0.71(3)	0.59(2)

extensions of the fibres and shows that relation (1) holds during deformation. The linear regression values are $e_3 = 240 \pm 10$ GN m^{-2} and $A = 0.26 \pm 0.01$ m^2 GN^{-1}.

The strain originates from the elastic extension of the polymer chains, ε_e, and from the elastic rotation of the chain or crystallite symmetry axis towards the fibre axis ε_r. The latter can be expressed as:

$$\varepsilon_r = \frac{\langle\cos\varphi\rangle - \langle\cos\varphi_0\rangle}{\langle\cos\varphi_0\rangle} \tag{3}$$

where φ_0 is the initial disorientation angle.

Introducing the variable $u = \langle\sin^2\varphi\rangle$, we may approximate (3) as:

$$\varepsilon_r = \frac{u_0 - u}{2} \tag{4}$$

The second term in (1) presents the rotational contribution to the elastic compliance:

$$\frac{d\varepsilon_r}{d\sigma} = Au \tag{5}$$

From equations (4) and (5) the relation between the stress and the orientation parameter u is obtained:

$$u = u_0\exp(-2A\sigma) \tag{6}$$

As shown in *Figure* 2, this exponential relation between u and σ is observed during the first and the second extension of the fibre. The experimental value for the parameter in the exponent, C, is for the second extension somewhat lower than for the first. Presumably plastic rotation of crystallites towards the fibre axis takes place in the first extension. This notion was also gained from a close examination of the tensile curves. For high strain rates these curves are slightly concave or almost straight. The increase of the first derivative for progressively larger strains is much less than that of the dynamic modulus E, as shown in *Figure* 4. For low strain rates even a slight drop in slope of the tensile curve near a strain of 0.4% is observed. Presumably in the first extension of the fibre an irreversible rotation of the crystallites occurs here. This would explain the increase of E as a result of a progressively narrowing of the crystallite orientation distribution with increasing strain.

For the analysis we now adopt a simplified approach by assuming that the total axial deformation in the first drawing cycle is made up of the elastic strain, ε_{er}, including extension and rotation of the crystallites, and of the irreversible rotational contribution ε_p. In the second cycle it is assumed that only elastic deformation of the crystallites occurs. As an analogy with equation (4) we can write ε_p as:

$$\varepsilon_p = \frac{u_0 - u_1}{2} \tag{7}$$

where u_1 is the value of the orientation parameter at the start of the second extension, i.e. after a maximum stress σ has been reached in the first extension. When the orientation parameter reaches the value u for a stress σ in the first drawing cycle, the increase in orientation is given by $(u_0 - u)$. Part of this difference is caused by elastic rotation of the crystallite axes according to:

$$u = u_1\exp(-C_2\sigma) \tag{8}$$

which describes the relationship between u and σ in the second extension. The remaining part arises from the irreversible rotation of the crystallites, which we presuppose to be expressed as:

$$u_0 - u_1 = u_0[1 - \exp(-\lambda\sigma)] \tag{9}$$

The parameter λ is introduced here for characterization of the plastic rotation and is dependent on the time. Since for the first extension:

$$u = u_0\exp(-C_1\sigma) \tag{10}$$

it follows that:

$$C_1 = C_2 + \lambda \tag{11}$$

The numerical results of the orientation *versus* stress measurement are given in *Table* 2. From these results values for λ ranging from 0 to 0.3 m^2 GN^{-1} are obtained.

For small values of $\lambda\sigma$ we derive from expression (7) and (9) that:

$$\varepsilon_p = \frac{1}{2}\lambda u_0\sigma \tag{12}$$

Figure 6 shows the residual deformation as a function of the previously applied stress, a linear relation is observed up to $\sigma \sim 0.7$ GN m^{-2}. With the values for u_0 given in *Table* 2 the values derived for λ are: 0.21, 0.27, 0.28 and 0.15 m^2 GN^{-1} for fibres 1 to 4. Although the precision is rather low, these λ values agree with those derived from equation (11). We note that there is a tendency for λ to be larger for the less oriented fibres.

By measuring the dynamic modulus as a function of σ during extension it is in principle possible to determine e_3 and C independently of the orientation measurements. From the expressions (1) and (10) the following relationship is derived:

$$\sigma = C^{-1}\ln\left[\frac{\frac{1}{E_0} - \frac{1}{e_3}}{\frac{1}{E} - \frac{1}{e_3}}\right] \tag{13}$$

Figure 7 shows the data observed in the first extension of the fibre, with $e_3 = 240$ GN m^{-1} as derived from *Figure* 5. A drop in the slope is observed near $\sigma \sim 0.8$ GN m^{-2}. The simultaneous determination of e_3 and C by regression analysis of the data up to this stress, yielded values with

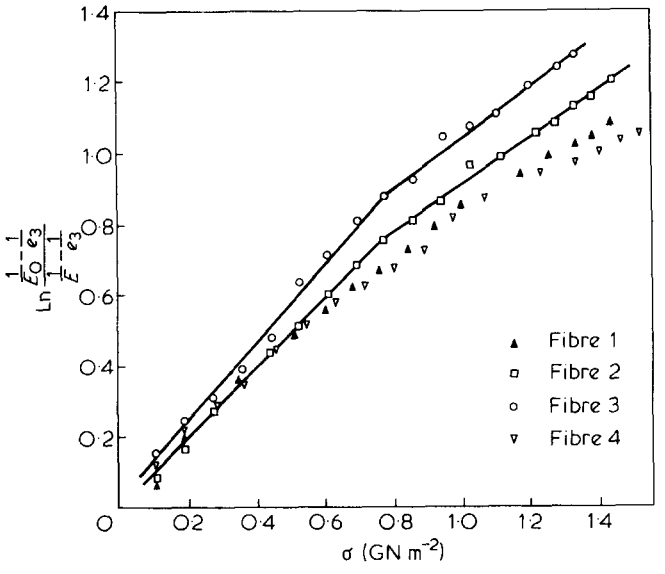

Figure 7 Dependence of

$$\ln\left[\left(\frac{1}{E_0}-\frac{1}{e_3}\right)\Big/\left(\frac{1}{E}-\frac{1}{e_3}\right)\right]$$

on the stress

large standard deviations: $e_3 = 245 \pm 30$ GN m^{-2} and $C_1 = 0.9 \pm 0.2$ m^2 GN^{-1}. This is due to the strong correlation between C and e_3. In addition, there are few observed moduli with values close to e_3. Thus, *Table* 2 gives the values for both slopes, C_1, C_2 and C_1' derived from regression using a fixed value $e_3 = 240$ GN m^{-2}. According to equation (13) the difference between the C values of the first and the second extension should be λ, which is indeed observed.

For a truly elastic rotation of crystallites during the second extension of the fibre, one would expect on the basis of equations (6) and (8) that

$$C_2 = 2A \tag{14}$$

Up to $\sigma \sim 0.8$ GN m^{-2} we observe that $C_2 > 2A$, though the difference tends to become smaller for the more perfectly oriented fibres. It can even be stated that for these fibres the two slopes in *Figure* 7 are not clearly resolved since the curve adopts a more or less convex shape. Now the constant C has been derived from experiments in which, by incremental loading, large amplitudes of rotation were imposed, whereas A has been obtained from measurements in which small amplitudes of rotation were applied. Presumably various relaxation processes accompany the rotation of crystallites towards the fibre axis, which results in an apparently lower force constant even during the second extension of the fibre. At large strains the orientation distribution becomes contracted which implies that only small amplitudes of rotation are possible. In this region of strain hardening characterized by the second slope C_1', we may expect therefore that C_1' approaches $2A$.

The total strain in the first extension of the fibre, excluding axial flow caused by a pure translationally-directed process, is given by:

$$\varepsilon = \frac{\sigma}{e_3} + 1/2(u_0 - u) \tag{15}$$

With equation (10) the strain can be expressed as a function of the orientation parameter u:

$$\varepsilon = \frac{1}{C_1 e_3}\ln\frac{u_0}{u} + 1/2(u_0 - u) \tag{16}$$

Figure 3 shows the observations and the calculated curves using the values for u_0 and C_1 given in *Table* 2.

Finally, from equations (10) and (15) the relationship between the strain and the stress is derived:

$$\varepsilon = \frac{\sigma}{e_3} + \frac{u_0}{2}[1 - \exp(-C_1\sigma)] \tag{17}$$

where the initial static modulus is given by:

$$E_s^{-1} = \frac{1}{e_3} + \frac{C_1 u_0}{2} \tag{18}$$

Using equation (18) we now calculate C with E_s from *Table* 1, u_0 from *Table* 2 and $e_3 = 240$ GN m^{-2} and find values ranging from 0.58 to 0.67 m^2 GN^{-1}.

Expression (17) may be regarded as a first approximation for the tensile curve of a fibril consisting of a linear arrangement of crystallites which have a narrow orientation distribution u_0 with respect to the fibril axis. The parameter C takes account of the rotation of the crystallites during deformation and includes the elastic, retarded elastic and irreversible contributions. *Figure* 8 shows the observed and two calculated tensile curves, e.g. for $u_0 = 0.048$ and $u_0 = 0.016$, using a single value $C = 0.7$ m^2 GN^{-1}. Presumably the differences observed at large ε are caused by the translationally directed flow, which also shows up in *Figure* 6 for $\sigma > 0.7$ GN m^{-2}.

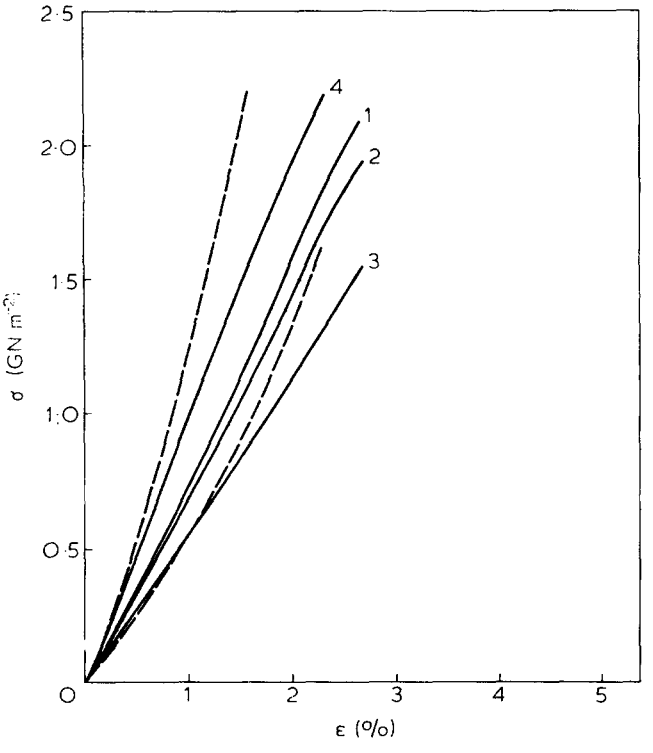

Figure 8 Tensile curves measured at a strain rate of 10% min^{-1}. Broken curves are computed for $u_0 = 0.016$ and $u_0 = 0.048$ with $C = 0.7$ m^2 GN^{-1} and $e_3 = 240$ GN m^{-2}

DISCUSSION

The preceding analysis has shown that the series model of crystallites can be applied successfully to the interpretation of the tensile deformation process of PpPTA fibres. Only three parameters determine the elastic deformation: the initial crystallite orientation distribution $\langle \sin^2 \varphi_0 \rangle$, the modulus of the polymer chain e_3, and the force constant A^{-1} governing the rotation of the crystallites. Due to the mechanical anisotropy of the PpPTA crystallites we may apply the approximation $A^{-1} = g$. From *Figure* 5 it was derived that $A^{-1} = 3.8$ GN m^{-2}, which is in good agreement with the theoretically estimated value 2.4 $< g <$ 5.7 GN m^{-2}, based on the bending force constant of the hydrogen bonds between adjacent chains[1]. The significance of the hydrogen bonds for the rotation of the crystallites can also be exemplified in a different way. In a body built up of parallel and undeformable rods, which make an angle with the stress direction, the rotation of the rods can only take place by a relative displacement of the rods. The motion is similar to that of a row of books when they are falling over. In case of the PpPTA fibres the relative displacement is controlled by the hydrogen bonds between the chains. In this respect it may be useful to determine the shear modulus of the fibre, $G = S_{44}^{-1}$. It can be shown that for medium and highly oriented fibres:

$$S_{44} = \frac{1}{g} + \left(\frac{3}{e_1} + \frac{2}{e_3} - \frac{5}{2g} + \frac{\nu_{12}}{e_1} + \frac{4\,\nu_{13}}{e_3} \right) \langle \sin^2 \varphi \rangle \qquad (19)$$

For highly oriented fibres $G = g$ which allows the determination of g directly.

While λ describes the irreversible rotation of the crystallites, the difference between C_2 and $2A$ is attributed to reversible flow processes during deformation. Both parameters, λ and C_2, tend to be larger for less perfectly oriented fibres. This suggests that crystallites with disorientation angles in the tail ends of the distribution show more rotational flow behaviour. This effect may be understood by realizing that in a fibre under axial tension the largest macroscopic shear stresses are found at an angle of 45° to the fibre axis. The weakest links in a PpPTA crystallite are between the rodlike chains; accordingly for increasing disorientation of the crystallite symmetry axis it is likely that the viscous part of the rotational motion becomes more pronounced.

Irreversible rotation of crystallites resulting in a set after the first extension, however, may also be caused by the removal of structural constraints like interfibrillar links. The presence of voids, as observed by small-angle X-ray scattering, is an important factor in this respect because the voids induce local stresses exceeding the macroscopic stress which may disrupt the interfibrillar links. Based upon space filling considerations it may be assumed that less perfectly oriented fibres have a larger amount of voids which results again in a larger set.

While the deformation in the first extension of the fibre is accompanied by irreversible rotation and for $\sigma > 0.8$ GN m^{-2} also by an irreversible extension of the crystallites, the deformation in the second cycle is almost completely reversible and shows only retarded elastic behaviour. The difference between the force constant for the rotational motion in the second cycle, $2C_2^{-1}$, and g tends to become smaller for the more perfectly oriented fibres. Above $\sigma \sim 0.8$ GN m^{-2} an increase of this force constant approaching the value of 3.8 GN m^{-2} is observed. We believe that this change in slope seen in *Figure* 7 and the rise in slope shown in *Figure* 6 at about the same stress is not merely coincidental. Presumably, the rotational flow has fallen away and axially, or translationally, directed flow starts to prevail. This is probably due to the fact that the highly contracted orientation distribution allows only small amplitudes of rotation for which the force constant approaches the value A^{-1} pertaining to the pure elastic rotation.

Since the deformation process is governed by the crystallite orienting mechanism, it is clear that the presence of structural irregularities, like impurities, will hamper the alignment of the fibrils along the stress direction. This effect will lead to premature rupture and thus to a lower fibre strength.

ACKNOWLEDGEMENT

The author acknowledges with thanks the many stimulating and helpful discussions with Dr J. J. van Aartsen and Mr F. Elkink, who also provided technical assistance. He is also grateful to Messrs H. Angad Gaur, H. A. Stuut and Dr H. de Vries for valuable suggestions.

REFERENCES

1 Northolt, M. G. and van Aartsen, J. J. *J. Polym. Sci. (Polym. Symp.)* 1978, **58**, 283
2 Dobb, M. G., Johnson, D. J. and Saville, B. P. *J. Poly. Sci. (Polym. Phys. Edn)* 1977, **15**, 2201
3 de Vries, H. and Weijland, H. G. *Text. Res. J.* 1958, **28**, 183